



## COVID-19 Research Tools

Defeat the SARS-CoV-2 Variants

InVivoGen

# The Journal of Immunology

RESEARCH ARTICLE | APRIL 15 2005

## Glucose Availability Regulates IFN- $\gamma$ Production and p70S6 Kinase Activation in CD8<sup>+</sup> Effector T Cells<sup>1</sup>

Candace M. Cham; ... et. al

*J Immunol* (2005) 174 (8): 4670–4677.

<https://doi.org/10.4049/jimmunol.174.8.4670>

### Related Content

Drak2 Is Upstream of p70S6 Kinase: Its Implication in Cytokine-Induced Islet Apoptosis, Diabetes, and Islet Transplantation

*J Immunol* (April,2009)

STAT5 Is Essential for Akt/p70S6 Kinase Activity during IL-2-Induced Lymphocyte Proliferation

*J Immunol* (October,2007)

Uncoupling p70<sup>S6</sup> Kinase Activation and Proliferation: Rapamycin-Resistant Proliferation of Human CD8<sup>+</sup> T Lymphocytes

*J Immunol* (March,2001)

# Glucose Availability Regulates IFN- $\gamma$ Production and p70S6 Kinase Activation in CD8<sup>+</sup> Effector T Cells<sup>1</sup>

Candace M. Cham<sup>\*†</sup> and Thomas F. Gajewski<sup>2\*†‡</sup>

**Differentiation of CD8<sup>+</sup> T cells from the naive to the effector state is accompanied by changes in basal gene expression profiles that parallel the acquisition of effector functions. Among these are metabolism genes, and we now show that 2C TCR transgenic effector CD8<sup>+</sup> T cells express higher levels of glycolytic enzymes and display greater glucose uptake, a higher glycolytic rate, and increased lactate production compared with naive cells. To determine whether glucose was required for effector T cell functions, we regulated glucose availability in vitro. Glucose deprivation strongly inhibited IFN- $\gamma$  gene expression, whereas IL-2 production was little affected. Inhibition correlated with diminished phosphorylation of p70S6 kinase and eIF4E binding protein 1 and a requirement for de novo protein synthesis, whereas other signaling pathways known to regulate IFN- $\gamma$  expression were unaffected. Together, our data reveal that optimal induction of IFN- $\gamma$  transcription is a glucose-dependent process, indicate that there are undefined factors that influence IFN- $\gamma$  expression, and have implications for regulation of the effector phase of CD8<sup>+</sup> T cell responses in tissue microenvironments. *The Journal of Immunology*, 2005, 174: 4670–4677.**

Post-thymic CD8<sup>+</sup> T cells that have not yet encountered specific Ag are considered naive and lack the ability to lyse target cells or secrete high levels of effector cytokines, such as IFN- $\gamma$ . TCR and costimulatory receptor engagement leads to IL-2 production, cell cycle progression, and acquisition of effector functions. Cell cycle progression appears to be necessary for the acquisition of lytic activity (1), suggesting that epigenetic modifications occur during proliferation that facilitate differentiation, as has been seen in CD4<sup>+</sup> T cells (2, 3). Although initial activation of naive CD8<sup>+</sup> T cells is thought to occur in secondary lymphoid organs through cross-presentation of Ag by host APCs, differentiated effector cells exit the lymph node and migrate to inflamed target tissues so as to be positioned to carry out Ag-specific effector functions. Thus, naive and effector CD8<sup>+</sup> T cells are dominantly activated in distinct tissue microenvironments.

One fundamental aspect of cellular regulation that may be particularly critical in vivo is the provision of metabolic substrates to support bioenergetics. In vitro, T cell activation is studied in culture medium supplemented with high concentrations of glucose and replete with an excess of amino acids and pyruvate, and is performed under an oxygen tension of 21%. However, these conditions might not always be approximated in vivo, and deficiencies in metabolic resources could significantly alter T cell function. The production of arginase and indoleamine-2,3-dioxygenase (IDO)<sup>3</sup> has been shown to deplete arginine and tryptophan, respectively, two amino acids that have been reported to be essential for T cell

function (4, 5). In vivo, the overexpression of arginase (6) or IDO (7, 8) by tumor cells has been implicated in the evasion of anti-tumor T cell responses. Thus, metabolic deviations can have negative impacts on immune responses.

Recently, the importance of glucose in T cell activation has been highlighted by the studies by Thompson et al. (9). They showed that CD28 costimulation stimulated glucose uptake and glycolysis via a PI3 kinase- and Akt-dependent pathway, arguing that one role of CD28 is to support the bioenergetic demands of activated T cells. There also is growing evidence that increased glucose metabolism is linked to protecting cells against apoptosis (10). Furthermore, growth factor deprivation leads to a drop in glycolysis, Glut1 expression, and intracellular ATP, all of which contribute to cell death (11, 12). However, although these pathways have been studied in tumor cell lines, and the aerobic glycolysis phenotype has been shown to contribute to the malignant state (13), little is known regarding the particular requirement for glucose-dependent metabolism for TCR signaling and effector functions in normal T lymphocytes.

To better understand differences between the naive and effector CD8<sup>+</sup> T cell differentiation states, we recently compared gene expression profiles using Affymetrix gene array analysis (14). We observed that eight genes encoding glycolytic enzymes were up-regulated in the effector state, suggesting that glucose-dependent metabolism might be important for regulating CD8<sup>+</sup> T cell effector function. In this study we show not only that CD8<sup>+</sup> T cell differentiation to the effector state is accompanied by marked up-regulation of glycolytic machinery, but that glucose is mandatory for a subset of signaling pathways and gene expression events. Our results have implications for the metabolic support of optimal T cell effector function in target tissue microenvironments, such as a growing solid tumor.

## Materials and Methods

### Mice

2C/RAG2<sup>-/-</sup> mice were bred in a specific pathogen-free animal facility at University of Chicago. C57BL/6J and DBA/2J mice were obtained from The Jackson Laboratory. Experimental procedures involving mice were approved by the institutional animal care and use committee at University of Chicago.

\*Committee on Cancer Biology, Departments of <sup>†</sup>Pathology and <sup>‡</sup>Medicine, University of Chicago, Chicago, IL 60637

Received for publication September 13, 2004. Accepted for publication January 31, 2005.

The costs of publication of this article were defrayed in part by the payment of page charges. This article must therefore be hereby marked *advertisement* in accordance with 18 U.S.C. Section 1734 solely to indicate this fact.

<sup>1</sup> This work was supported by the National Institutes of Health (R01AI47919) and a Burroughs Wellcome Fund Translational Research Grant.

<sup>2</sup> Address correspondence and reprint requests to Dr. Thomas F. Gajewski, University of Chicago, MC2115, 5841 South Maryland Avenue, Chicago, IL 60637. E-mail address: tgajewsk@medicine.bsd.uchicago.edu

<sup>3</sup> Abbreviations used in this paper: IDO, indoleamine-2,3-dioxygenase; ATF, activating transcription factor; 2-DG, 2-deoxy-D-glucose; 4E-BP1, eIF4E binding protein 1; RPA, RNase protection assay; S6K, p70S6 kinase.

### Cells and media

The generation of effector 2C TCR transgenic CD8<sup>+</sup> T cells has been described previously (14). Briefly, naive 2C cells were purified from the spleens of 2C/RAG2<sup>-/-</sup> mice using the StemSep Enrichment Cocktail for murine CD8<sup>+</sup> T cells (Stem Cell Technologies). To generate effector cells, naive cells were plated with mitomycin C-treated P815-B7.1 cells for 4 days. On the fourth day of stimulation, the cells were collected, subjected to Ficoll-Hypaque centrifugation, and reprimed for another 4 days to generate day 8 effector cells. Day 8 cells have the ability to secrete effector cytokines and lyse Ag-expressing target cells (data not shown).

Nutrient-free DMEM was made with DME Base (Sigma-Aldrich). This minimal solution was supplemented with 3.7 g/L NaHCO<sub>3</sub> and 15 mg/L phenol red. The pH was adjusted to 7.2. FCS was dialyzed against nutrient-free DMEM using 12K-14K MWCO Spectra/Por 2 dialysis tubing (Spectrum Laboratories). Both nutrient-free DMEM and dialyzed FCS tested negative for glucose on a Diastix glucose dipstick (Bayer). Every experiment using nutrient-free DMEM contained 10% dialyzed FCS. Where indicated, D-glucose (Sigma-Aldrich) was supplemented in nutrient-free DMEM. Alternatively, 2-deoxy-D-glucose (2-DG; Sigma-Aldrich) was added at the indicated concentrations to high glucose DMEM (Invitrogen Life Technologies) containing 25 mM glucose and 10% undialyzed FCS.

### Mixed lymphocyte reaction

To activate bulk T cells, 6 × 10<sup>6</sup> splenocytes from C57BL/6J mice were cocultured with 6 × 10<sup>6</sup> irradiated splenocytes (2000 rad) from DBA/2J mice in each well of a 24-well plate. After 5 days, cells were collected and subjected to Ficoll-Hypaque centrifugation. Viable cells were counted using trypan blue exclusion.

### Glucose uptake assay

Cells were washed in PBS before incubation for 15 min at 37°C in glucose uptake buffer (8.1 mM Na<sub>2</sub>HPO<sub>4</sub>, 1.4 mM KH<sub>2</sub>PO<sub>4</sub>, 0.5 mM MgCl<sub>2</sub>, 2.6 mM KCl, 136 mM NaCl, and 0.9 mM CaCl<sub>2</sub>, pH 7.4) at a density of 2 × 10<sup>6</sup> cells/0.1 ml. 2-[1,2-(N)-<sup>3</sup>H]2-deoxy-D-glucose (PerkinElmer; 1 mCi/ml) was diluted 1/50 in glucose uptake buffer. Twenty-five microliters of a 20% perchloric acid (Sigma-Aldrich)/8% sucrose solution was added to the bottom of a 0.5-ml microfuge tube. 1-Bromododecane (200 μl; Sigma-Aldrich) was overlaid above the perchloric acid/sucrose solution. Fifty microliters of [<sup>3</sup>H]2-DG (20 μCi/ml) was overlaid above the 1-bromododecane layer. After the 37°C incubation, 100 μl of cells was added to the DOG layer and pulsed for various lengths of time. The reaction was stopped by centrifugation at 14,000 rpm for 10 min. Tubes were then snap-frozen in an ethanol/dry ice bath. Using a microfuge cutter, the tips of the tubes were cut just above the perchloric acid/sucrose/bromododecane interface and transferred into scintillation vials containing 250 μl of 1% Triton X-100. Cytosint (ICN; 2 ml) was added to each vial and counted using an LS6500 scintillation counter (Beckman Coulter). Each sample was measured in triplicate. Statistical analysis (*t* test) was performed using Microsoft Excel.

### Glycolysis assay

Measurement of glycolysis is based on the generation and diffusion of [<sup>3</sup>H]<sub>2</sub>O during the dehydration reaction mediated by enolase. The glycolytic rate is calculated from the ratio of diffused to undiffused radioactivity. Briefly, 10<sup>6</sup> cells were washed with PBS and preincubated in Krebs buffer (115 mM NaCl, 2 mM KCl, 25 mM NaHCO<sub>3</sub>, 2 mM CaCl<sub>2</sub>, 0.25% BSA, and 1 mM MgCl<sub>2</sub>) for 30 min at 37°C under a 5% CO<sub>2</sub> atmosphere. Cells were pelleted, resuspended in 0.5 ml of prewarmed 25 mM glucose/Krebs buffer, and pulsed with 10 μCi of D-[5-(N)-<sup>3</sup>H]glucose (PerkinElmer) for exactly 1 h at 37°C in 5% CO<sub>2</sub>. As controls, cell-free samples (background fraction) and 1 μCi of [<sup>3</sup>H]<sub>2</sub>O (PerkinElmer) in 0.2 ml of Krebs buffer (diffusion fraction) were included. Triplicate samples were lysed with 0.2 N HCl in uncapped PCR tubes. Each tube was placed in a scintillation vial containing 0.5 ml of H<sub>2</sub>O (diffused sample). Vials were tightly capped and sealed. After ≥48 h of diffusion, each tube was transferred to a fresh scintillation vial containing 0.5 ml of H<sub>2</sub>O and 0.1 N HCl (undiffused sample). Scintillation mixture was added to each vial, and samples were counted for 1 min on an LS6500 scintillation counter. The following formula was used to calculate the glycolytic rate:  $((\text{sample}^{\text{diff}} - \text{frac}^{\text{bkgd}}) / \text{frac}^{\text{diff}}) \times (12,500) = \text{nmol glucose}/10^6 \text{ cells/h}$ . Statistical analysis (*t* test) was performed using Microsoft Excel.

### Lactate assay

Lactate produced from cells stimulated for 24 h was determined from supernatant using lactate reagent (Sigma-Aldrich; 5 μl of cell supernatant in 0.2 ml of lactate reagent). Concentrations were determined based on lactate

standard (Sigma-Aldrich). Statistical analysis (*t* test) was performed using Microsoft Excel.

### SDS-PAGE and Western blotting

In each well of a six-well plate, 2.5 × 10<sup>6</sup> cells were stimulated with 12.5 × 10<sup>6</sup> sheep anti-mouse IgG-conjugated polystyrene beads (DynaL Biotech) coated with anti-CD3 (2C11; 1 μg/ml) and anti-CD28 (PV-1; 1 μg/ml) Abs for the indicated number of hours. Cells were lysed as described by Cham et al. (14). For unstimulated cells, 2.5 × 10<sup>6</sup> naive or day 8 effector 2C cells were immediately lysed after collection. Cytosolic lysates from 2.5 × 10<sup>6</sup> naive and primed 2C/RAG2<sup>-/-</sup> CD8<sup>+</sup> T cells were subjected to SDS-PAGE on 10–12% acrylamide gels.

Proteins were transferred onto Immobilon-P membranes (Millipore) and blocked with 5% BSA or milk in TBST. For immunoblotting, polyclonal Abs were diluted 1/250 and mAbs were diluted 1/500 to 1/1000 with 1% BSA in TBST. Abs against phospho-Thr<sup>389</sup> S6 p70 kinase 1 (S6K1), total S6K1, phospho-Thr<sup>3746</sup> eIF4E binding protein 1 (4E-BP1), phospho-ERK, and phospho-p38 MAPK were obtained from Cell Signaling Technology. Anti-phospho-Thr<sup>421</sup>/Ser<sup>424</sup> S6K1 Ab was purchased from Sigma-Aldrich, and anti-phospho-JNK Ab was obtained from Promega. Ab against total ERK was purchased from Zymed Laboratories, Ab against total JNK was obtained from BD Pharmingen, and Ab against total p38 MAPK was obtained from Santa Cruz Biotechnology. Individual bands were quantified using UN-SCAN-IT software (Silk Scientific) and were normalized against a loading control. Statistical analysis (paired *t* test) was performed using Microsoft Excel.

### Cytokine ELISAs

To evaluate cytokine production, 10<sup>5</sup> purified day 8 effector 2C CD8<sup>+</sup> T cells, L3C5 CD8<sup>+</sup> T cells, or activated C57BL/6 T cells were stimulated with 5 × 10<sup>5</sup> polystyrene beads (DynaL Biotech) coated with anti-CD3 (2C11; 1 μg/ml) and anti-CD28 (PV-1; 1 μg/ml) Abs in 96-well, flat-bottom plates for ~20 h at 37°C. For APC stimulation, 5 × 10<sup>5</sup> mitomycin C-treated P815 mastocytoma cells transfected with B7.1 (P815-B7.1) were used to stimulate 10<sup>5</sup> 2C cells. For other stimulations, PMA (50 ng/ml) and ionomycin (0.5 μg/ml) or IL-12 (10 ng/ml) and IL-18 (0.5 μg/ml) were used to stimulate 10<sup>5</sup> 2C cells. Supernatants were collected after 20 h of stimulation and analyzed for IL-2 or IFN-γ by ELISA using Ab pairs from BD Pharmingen. Statistical analysis (paired *t* test) was performed using Microsoft Excel.

### Assessment of apoptosis

Survival rates of T cells stimulated for 24 h under glucose-depriving conditions were determined by dual annexin V-FITC (BD Pharmingen) and propidium iodide staining. T cells (10<sup>6</sup>) were stimulated for 24 h with beads coated with 2C11 and PV-1, as described above, in a 24-well plate. Staining was conducted according to the manufacturer's instructions. Survival rate was assessed by the percentage of cells that stained negatively for both annexin V and propidium iodide, as determined by flow cytometry.

### RNase protection assays (RPA)

Total RNA was extracted from cells using TRIzol (Invitrogen Life Technologies). To analyze cytokine mRNA, 1 μg of total RNA was used in the BD RiboQuant MultiProbe System (mCK-1; BD Pharmingen) according to the manufacturer's instructions. To analyze mRNA stability, actinomycin D (5 μg/ml) was added to cells after 4 h of stimulation (time zero). Individual bands were quantified using UN-SCAN-IT software (Silk Scientific) and were normalized against a loading control. Statistical analysis (paired *t* test) was performed using Microsoft Excel.

### Gel shift analysis

Effector cells (2.5 × 10<sup>6</sup>) were stimulated with 12.5 × 10<sup>6</sup> beads as described above for the indicated times. Nuclei were isolated from 5 × 10<sup>6</sup> stimulated effector cells, according to the method described by Schreiber et al. (15), with slight modifications. The protein content of nuclear extracts was measured using a DC Protein Assay kit (Bio-Rad). Approximately 5 μg of protein was used for each analysis. The following sequences were used as probes to detect DNA binding activity (5'→3'): *OCT-1(a)*, GATCTGTGCAATGCAAACTACTAGAA; *OCT-1(b)*, GATCTTCTAGTGATTTGCATTCGACA; *AP-1(a)*, GATCCGCTTGATGACTCAGCCG GAA; *AP-1(b)*, GATCTCCGGCTGAGTCATCAAGCG; activating transcription factor-2(a) (*ATF-2*), GATCGATCCGGCTGACGTCATCAAGC TA; *ATF-2(b)*, GATCTAGCTTGATGACGTCAGCCGGATC; *NFAT(a)*, CCCAAAGAGGAAAATTTGTTTCATACAG; *NFAT(b)*, GCCTTCTG TATGAAACAAATTTCTCTCT; *NF-κB(a)*, GATCCAACGGCAGGGG

AATCCCCTCTCCTTA; and *NF-κB(b)*, GATCTAAGGAGAGGGGA ATTCCCCTGCCGTTG.

Probes were designed with overhang sequences for radiolabeling purposes. Complementary single-stranded oligonucleotides were annealed in TEN buffer (100 mM Tris (pH 7.6), 10 mM EDTA (pH 8), and 1 M NaCl). Double-stranded probes (100 ng) were labeled 30 μCi of each [<sup>32</sup>P]dNTP and Klenow fragment (New England Biolabs). Unincorporated nucleotides were removed with Quick Spin G-25 columns (Roche); 10<sup>5</sup> cpm/ml was used in each reaction. Protein-DNA complexes were resolved on a 6% native gel, dried, and exposed to film. Individual bands were quantified using UN-SCAN-IT software (Silk Scientific) and were normalized against a loading control. Statistical analysis (paired *t* test) was performed using Microsoft Excel.

### Semiquantitative RT-PCR

Effector 2C T cells were stimulated in the presence or the absence of 2-DG with 2C11/PV-1-coated beads, as described above, for 6 or 12 h. RNA was isolated and converted to cDNA. Serial dilutions (1/5) of cDNA were used as templates for RT-PCR. Actin mRNA was used as a loading control. The primers used were: T-bet(*a*), AACAGCATCGTTTCTTCTATCCC; T-bet(*b*), TCTGGGTGGACATATAAGCGGTT; Eomesodermin(*a*), GTT TCCTTCTTGAGCTCAA; and Eomesodermin(*b*), CATGGAATCGT AGTTGTCCC.

## Results

### Glycolytic machinery is up-regulated in effector 2C CD8<sup>+</sup> T cells

Our previous gene array screen revealed that mRNA expression of aldolase C and α-enolase were both greater in effector 2C CD8<sup>+</sup> T cells compared with naive 2C cells (14). To determine whether glycolytic enzymes were increased at the protein level in effector 2C CD8<sup>+</sup> T cells compared with naive 2C cells, Western blot analysis was performed. The expression of aldolase C and α-enolase was substantially higher in effector cells, whereas β-actin was expressed comparably (Fig. 1A).

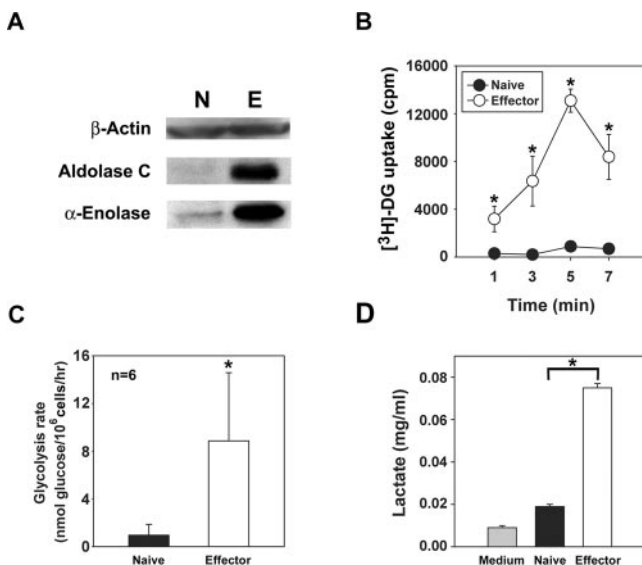


**FIGURE 1.** Effector 2C CD8<sup>+</sup> T cells have increased protein expression of glycolytic enzymes and increased glucose-dependent metabolism. *A*, Effector cells express higher protein levels of glycolytic enzymes, aldolase C, and α-enolase, as determined by Western blotting. Expression of actin was used as an indicator of equivalent loading. *B*, Resting effector cells have greater glucose uptake compared with naive cells. The rate of glucose uptake was determined by the amount of [1,2-<sup>3</sup>H]-2-DG (cpm) in each sample. Data are representative of at least three independent experiments. Statistics compare naive vs effector T cells. *C*, Effector cells have a higher glycolytic rate compared with naive cells. *D*, Stimulated effector cells produce significant levels of lactate. Similar results were observed in at least two independent experiments. \*, *p* < 0.05.

To explore glucose-dependent metabolism in these differentiation states, [<sup>3</sup>H]2-DG uptake was measured. CD8<sup>+</sup> effector cells showed markedly increased uptake of [<sup>3</sup>H]2-DG compared with naive cells (Fig. 1B). Similarly, the glycolytic rate was substantially higher in effector cells (Fig. 1C). The conversion of pyruvate to lactate enables cells to generate additional ATP from glucose without dependence on oxygen. To determine whether glucose was predominantly being metabolized anaerobically, we measured lactate production released into the supernatant. In resting cells, lactate production was undetectable (data not shown). However, lactate generation after stimulation with anti-CD3 and anti-CD28 Abs was readily detected from effector 2C cells, whereas that detected from naive cells was little above background (Fig. 1D). Together, these results indicate that glucose-dependent metabolism is markedly up-regulated in CD8<sup>+</sup> effector T cells, and that this glucose is used, at least in part, anaerobically.

### IFN-γ, but not IL-2, production is preferentially inhibited by glucose deprivation

We hypothesized that glucose might be essential for a subset of functions unique to effector cells. Specifically, we reasoned that production of IFN-γ (made at significantly higher levels by effector cells) might be inhibited by limiting glucose availability, whereas production of IL-2 (made by both naive and effector cells) might be unaffected. Glucose deprivation was achieved in two ways. First, glucose- and pyruvate-free DMEM was used as a base and was supplemented with 10% FCS (dialyzed against glucose- and pyruvate-free DMEM) and D-glucose in varying amounts up to 25 mM. IFN-γ production from anti-CD3- and anti-CD28 Ab-stimulated effector CD8<sup>+</sup> T cells declined to an average of 17% of normal (*n* = 4) as the glucose concentration decreased (Fig. 2A). In contrast, IL-2 production was resistant to glucose deprivation (100% of normal, on the average; *n* = 4). Therefore, IFN-γ production was more sensitive to glucose deprivation than was IL-2 production (*p* = 0.0005). Second, 2-DG, an analog of glucose that blocks hexokinase, phosphoglucose isomerase, and phosphoglucose mutase (16), was added to DMEM containing 25 mM D-glucose. IFN-γ production also was more sensitive than IL-2 production to inhibition by 2-DG when stimulated with either anti-CD3 and anti-CD28 mAbs (Fig. 2B) or P815-B7.1 cells as APCs (Fig. 2C).

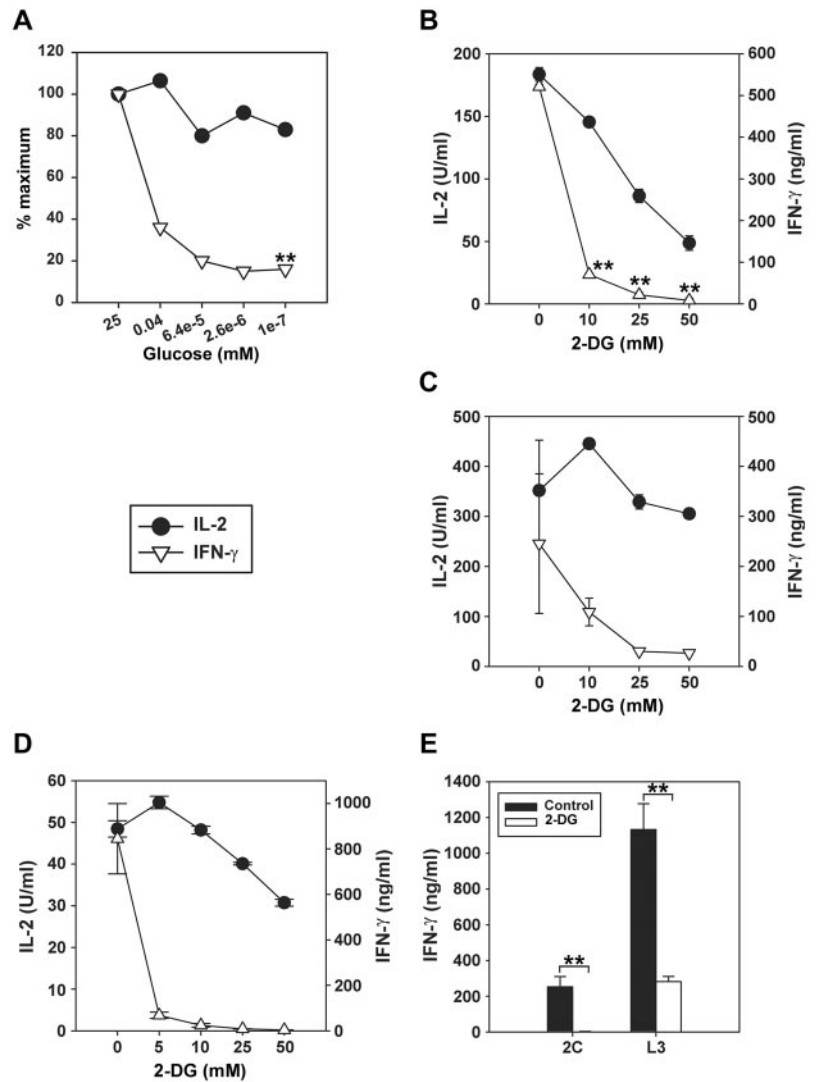
To determine that this preferential inhibition was not unique to primed 2C TCR transgenic T cells, bulk T cells collected from an MLR and a long-term CTL clone were analyzed. The same preferential inhibition of IFN-γ production over IL-2 production was observed by bulk T cells stimulated with anti-CD3- and anti-CD28 Ab-coated beads (Fig. 2D). Additionally, IFN-γ production by the CD8<sup>+</sup> CTL clone L3 (17) in response to the same stimulus was inhibited by 2-DG (Fig. 2E).

It was conceivable that stimulating T cells under glucose-depriving conditions may have caused the cells to undergo apoptosis. In our system, after 24 h of stimulation, cell death (as assessed by dual staining with annexin V and propidium iodide) in the absence of glucose (25 mM glucose, 52%; 0 mM glucose, 56%) or in the presence of 2-DG (0 mM 2-DG, 45%; 50 mM 2-DG, 46%) was not increased and did not account for the decrease in the production of select cytokines. Together, these results indicate that IFN-γ production by CD8<sup>+</sup> effector T cells is more dependent on glucose than is IL-2 production.

### Glucose deprivation affects IFN-γ gene transcription

It was of interest to determine the mechanism by which glucose deprivation was inhibiting IFN-γ production. To determine whether a proximal TCR signaling defect could be implicated, PMA and ionomycin were used to stimulate cytokine production.

**FIGURE 2.** IFN- $\gamma$  production is more sensitive to glucose depletion than IL-2 production. **A**, Effector 2C CD8<sup>+</sup> T cells were stimulated with anti-CD3 and anti-CD28 Ab-coated beads in glucose-free DMEM/10% dialyzed FCS with varying amounts of supplemented D-glucose. Cytokine production was determined by ELISA. Data are representative of six independent experiments. Paired *t* test was performed, comparing the ratios of IL-2/IFN- $\gamma$  production under 25 or 0–10<sup>-7</sup> mM glucose conditions. \*\*, *p* < 0.01. **B**, Effector cells were stimulated in high glucose (25 mM) DMEM/10% FCS containing the indicated amounts of 2-DG. Cytokine production was determined by ELISA. Data are representative of 13 independent experiments. Paired *t* test was performed, comparing the ratios of IL-2/IFN- $\gamma$  production under 25 or 0 mM glucose conditions. \*\*, *p* < 0.01. **C**, Effector 2C T cells were stimulated with mitomycin C-treated P815-B7.1 cells to stimulate cytokine production in the presence of 2-DG. Cytokine production was determined by ELISA. **D**, Activated C57BL/6 cells generated from a 5-day MLR were stimulated with anti-CD3 and anti-CD28 Ab-coated beads in varying amounts of 2-DG. Cytokine production was determined by ELISA. Data are representative of two independent experiments. **E**, L3 CD8<sup>+</sup> T cell clones were stimulated with anti-CD3 and anti-CD28 Ab-coated beads in 50 mM 2-DG. Cytokine production was determined by ELISA. All data are representative of at least three independent experiments. Paired *t* test was performed, comparing IFN- $\gamma$  production under 25 or 0 mM glucose conditions. \*\*, *p* < 0.01.



However, IFN- $\gamma$  production in response to PMA and ionomycin was still blocked by elimination of glucose from the medium (Fig. 3A) or with 2-DG (data not shown). As with the other stimuli, IL-2 production in response to PMA and ionomycin was little affected by glucose deprivation.

An alternative physiologic stimulus for inducing IFN- $\gamma$  production by T cells is the combination of the cytokines IL-12 and IL-18 (18). Signaling through IL-12R and IL-18R uses distinct proximal pathways from TCR signaling, converging at the point of p38 MAPK and NF- $\kappa$ B (19). Increasing amounts of 2-DG also inhibited IFN- $\gamma$  production induced by IL-12 and IL-18 (Fig. 3B). Collectively, these results suggest that a distal process downstream from TCR and CD28 that is not important for IL-2 production and is probably shared with the IL-12R/IL-18R pathways is sensitive to limitations in glucose availability.

To determine at what level IFN- $\gamma$  production was being affected by glucose deprivation, IL-2 and IFN- $\gamma$  mRNA were examined by RPA. Stimulation for 6 h with anti-CD3- and anti-CD28-coated beads in the absence of glucose revealed diminished levels of IFN- $\gamma$  mRNA, but minimal change in IL-2 mRNA (Fig. 3C). Kinetic analysis revealed that early induction of IFN- $\gamma$  mRNA was intact, but the levels began to decrease 4–7 h after stimulation in the presence of 2-DG, suggesting that IFN- $\gamma$  mRNA expression was not being sustained (Fig. 3D). After only 6–7 h, IFN- $\gamma$  mRNA levels in control-stimulated cells were already (on the average)

twice as abundant compared with IFN- $\gamma$  mRNA levels in glucose-deprived cells (*p* = 0.009; including *n* (glucose-free) = 2 and *n* (2-DG) = 4). This difference became even more striking at later time points.

Because decreased mRNA levels could be a result of decreased transcription or increased degradation, we used actinomycin D to block further transcription and assessed the half-life of IFN- $\gamma$  transcripts in the presence or absence of 2-DG. Actinomycin D was added 4 h after stimulation, and cells were harvested at various times for mRNA analysis by RPA. We observed that the rate of IFN- $\gamma$  mRNA decay followed the same kinetics with or without addition of 2-DG (Fig. 3E). This indicates that IFN- $\gamma$  mRNA degradation was not augmented by glucose deprivation, implying an effect at the level of diminished transcription.

#### Glucose deprivation does not inhibit factors known to regulate IFN- $\gamma$

TCR/CD28 engagement initiates multiple signaling pathways resulting in the activation of transcription factors that promote cytokine gene expression. The inhibitory effect of glucose deprivation on IFN- $\gamma$  production in response to PMA and ionomycin focused attention on downstream effectors. In particular, p38 MAPK has been reported to be critical for IFN- $\gamma$  production (20), and the p38 MAPK inhibitor SB203580 selectively blocked the production of IFN- $\gamma$ , but not that of IL-2, by primed 2C CD8<sup>+</sup> T

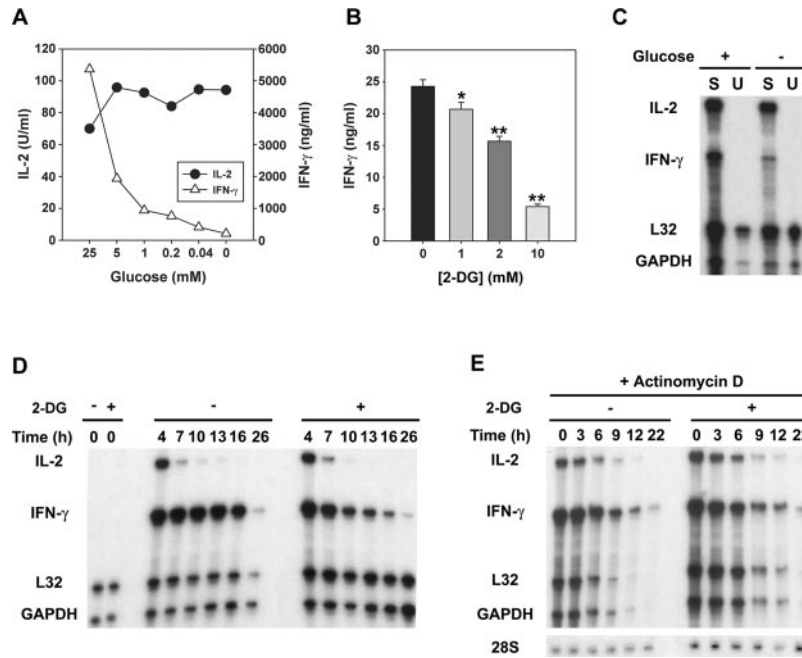
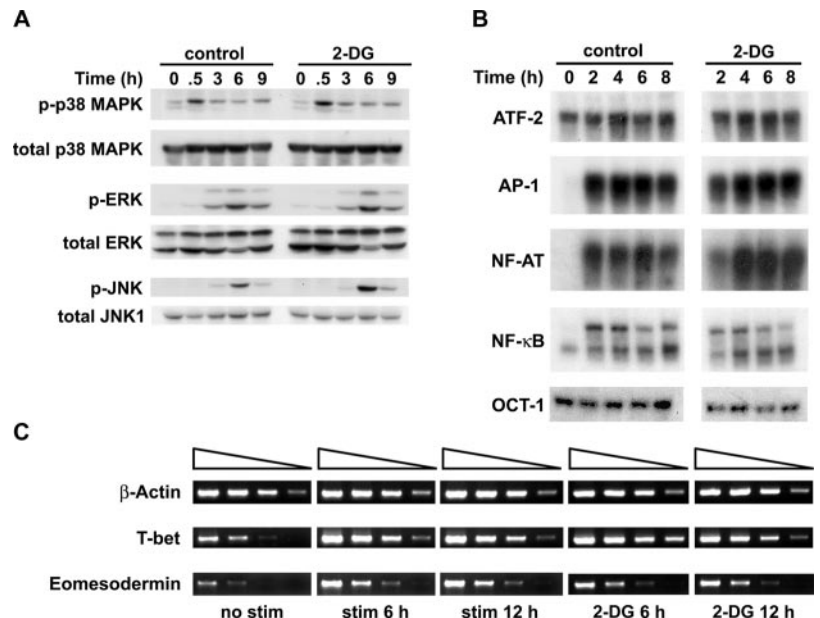


**FIGURE 3.** 2-DG inhibits IFN- $\gamma$  production at the level of mRNA. *A*, To bypass proximal TCR signaling, PMA and ionomycin were used to stimulate effector 2C CD8<sup>+</sup> T cells in glucose-free DMEM/10% dialyzed FCS containing varying amounts of D-glucose. Cytokine production was determined by ELISA. Data are representative of three independent experiments. *B*, IL-12 and IL-18 were used to induce IFN- $\gamma$  production by effector 2C T cells in the presence of 2-DG. Cytokine production was assayed by ELISA. Data are representative of at least three independent experiments. \*,  $p < 0.05$ ; \*\*,  $p < 0.01$ . *C*, Effector 2C T cells were stimulated in glucose-free DMEM/10% dialyzed FCS with (+) or without (-) supplemented 25 mM D-glucose. *S*, stimulated; *U*, unstimulated. After 6 h, total RNA was isolated and used to assess steady-state cytokine mRNA levels by RPA. Data are representative of two independent experiments. *D*, Effector 2C T cells were stimulated in complete DMEM/10% FCS with or without 2-DG for the indicated times. RNA was isolated and analyzed by RPA. Data are representative of four independent experiments. *E*, To determine whether 2-DG affected cytokine mRNA stability, effector 2C CD8<sup>+</sup> T cells were stimulated as described in *D*. After 4 h of stimulation, actinomycin D was added (time zero). Cells were collected at the indicated times after the addition of actinomycin D. RNA was isolated and analyzed by RPA. At extended time points, L32 and GAPDH mRNA also diminished; therefore, 28S mRNA was used as a loading control. Data are representative of two independent experiments.

cells (data not shown). However, phosphorylation of p38 MAPK (Fig. 4A) as well as the upstream activators MAPK kinase 3/MAPK kinase 6 (data not shown) was not inhibited by 2-DG ( $p = 0.5$ , at 3 h). Similarly, induction of phosphorylation of the other MAPKs, ERK and JNK, was unaffected (pERK,  $p = 0.6$ , at 3 h; pJNK,  $p = 0.5$ , at 3 h; Fig. 4A).

A key downstream target of p38 MAPK is ATF-2, a binding site for which has been described in the IFN- $\gamma$  promoter (21). Therefore, we assessed ATF-2 binding activity using labeled oligonucleotides containing a consensus ATF-2/cAMP response element binding site. ATF-2 binding activity was detected in the nucleus of both control and 2-DG-treated effector CD8<sup>+</sup> T cells 6 h after

**FIGURE 4.** Activation of MAPKs and DNA binding activity of transcription factors defined to regulate IFN- $\gamma$  gene expression in effector CD8<sup>+</sup> T cells are unaffected by 2-DG. *A*, To address whether glucose deprivation affects activation of MAPKs, effector cells were stimulated in the presence (50 mM) or the absence of 2-DG for the indicated time periods. Whole cell lysates were then prepared to examine kinase activity by Western blotting using phospho-specific Abs. Data are representative of at least four independent experiments. *B*, Effector cells were stimulated in the presence (25 mM) or the absence of 2-DG for the indicated time periods. Nuclear lysates were then prepared to examine transcription factor DNA binding activity by gel-shift analysis. Gel shifts using an OCT-1 probe were performed as an indicator of protein loading. IFN- $\gamma$  production was undetectable from cells stimulated in 25 mM 2-DG (data not shown). Data are representative of at least three independent experiments. *C*, mRNA levels of T-bet and eomesodermin were still induced despite the presence of 2-DG. Transcript levels were determined by semiquantitative RT-PCR.



activation ( $p = 0.1$ , at 4 h; Fig. 4B). In addition, AP-1 binding activity was not significantly changed in the presence of 2-DG ( $p = 0.1$ , at 4 h).

Other transcription factors have been implicated in regulating the IFN- $\gamma$  gene. Gel-shift analysis was performed to analyze the activities of NF- $\kappa$ B and NF-AT, each of which was induced after stimulation with anti-CD3/anti-CD28 Abs and was relatively unaffected by 2-DG (at 4 h: NF- $\kappa$ B,  $p = 0.3$ ; NF-AT,  $p = 0.5$ ; Fig. 4B). Additionally, STAT4 DNA binding activity was still present even in cells stimulated under 2-DG conditions (data not shown). Moreover, mRNA induction of the T-box family transcription factors T-bet and eomesodermin was not affected by 2-DG (Fig. 4C). Thus, we could find no evidence that the transcription factors known to regulate the IFN- $\gamma$  gene in CD8<sup>+</sup> T cells were inhibited by glucose deprivation.

#### 2-DG inhibits phosphorylation of p70S6K and 4E-BP1

We next considered a model in which an uncharacterized putative regulator might be required for maintaining long-term IFN- $\gamma$  transcriptional activity. In mammalian cells, protein synthesis can be regulated by the kinase, mammalian target of rapamycin, and its substrates, p70S6K and 4E-BP1. Recent work has suggested that activation of these kinases is dependent on nutrient availability in HEK293 cells (22). We investigated whether p70S6K was activated in effector 2C cells and whether this activation was inhibited by 2-DG. Phosphorylation of p70S6K was induced by anti-CD3 Ab alone, and this phosphorylation was not induced further by anti-CD28 Ab (data not shown). Interestingly, the addition of

2-DG inhibited p70S6K phosphorylation in a dose-dependent fashion (Fig. 5A). By contrast, phosphorylation of neither the related ribosomal kinase p90RSK nor ERK was inhibited. Kinetic analysis revealed that peak phosphorylation of p70S6K occurred 3 h after stimulation; this phosphorylation was delayed and reduced with 2-DG ( $p = 0.04$ ;  $n = 4$ ; Fig. 5B). 2-DG treatment also resulted in delayed phosphorylation of 4E-BP1 (Fig. 5B). Thus, phosphorylation of p70S6K and 4E-BP1, but not that of multiple additional kinases activated downstream from TCR engagement, was suppressed by glucose deprivation.

Because p70S6K is involved in regulated protein translation, we explored the possibility that de novo protein synthesis was required for the expression of the IFN- $\gamma$  gene, but not the IL-2 gene. To address this possibility, effector 2C cells were stimulated with anti-CD3 and anti-CD28 Abs in the presence or the absence of cycloheximide, and IL-2 and IFN- $\gamma$  mRNA levels were assessed by RPA. Interestingly, addition of cycloheximide at the time of stimulation almost completely inhibited IFN- $\gamma$  mRNA induction ( $p = 0.02$ ;  $n = 3$ ; Fig. 5C). By striking contrast, cycloheximide did not inhibit, but, rather, modestly potentiated IL-2 mRNA levels over time ( $p = 0.26$ ;  $n = 3$ ). To determine at what time point protein synthesis is required for IFN- $\gamma$  transcription, cycloheximide was added at various times during a 14-h stimulation. Addition of cycloheximide at early time points (2–6 h) after stimulation blocked further IFN- $\gamma$  transcription, but addition at later times had a minimal effect (Fig. 5D). These results indicate that a new protein intermediate must be produced during the first few hours downstream from CD3/CD28 stimulation for optimal IFN- $\gamma$  gene transcription in CD8<sup>+</sup> T cells.

## Discussion

Our current results underscore the particular importance of glucose for CD8<sup>+</sup> effector T cells. We observed that glucose-dependent metabolism is critical for IFN- $\gamma$ , but not IL-2, production, the latter cytokine being produced by both naive and effector T cells. Other aspects of glucose-dependent metabolism in hemopoietic cells have been reported. Frauwrith et al. (23) reported that glucose use was induced by CD28 costimulation. Growth factor withdrawal resulted in rapid down-regulation of the glucose transporter Glut1, which was also linked to cell death (11, 12). In addition, glucokinase was found in a multimeric complex with the proapoptotic Bcl-2 family member BAD in hepatocytes (10). Collectively, these observations establish a connection between glucose metabolism and regulated apoptotic death. Although we did not observe increased apoptosis in our model under conditions of glucose deprivation after 24 h, this may be because of concomitant CD28 costimulation that up-regulates expression of antiapoptotic molecules (24). Prolonged exposure to glucose-free conditions for >48 h did begin to result in increased apoptosis in primed 2C cells (data not shown). However, increased cell death did not explain the short term effects of glucose deprivation observed in our current study.

Although previous experiments have shown high glucose use by PHA-stimulated peripheral T cells (25), our current results show high glucose-dependent metabolism in resting (nonproliferating) effector cells, dissociating the glucose-dependent phenotype from the process of proliferation.

2-DG has been studied for physiological and metabolic effects in animals. 2-DG has been reported to induce multiple metabolic changes, including hyperglycemia (26), and increased production of oxytocin (27) and norepinephrine (28). In vivo administration of 2-DG has been shown to inhibit secretion of IFN- $\gamma$ , TNF- $\alpha$ , IL-1 $\beta$ , and IL-6, whereas production of IL-2 and IL-4 was not affected (29). In another report, Miller et al. (30) demonstrated that 2-DG can actually improve resistance to *Listeria monocytogenes* in mice.

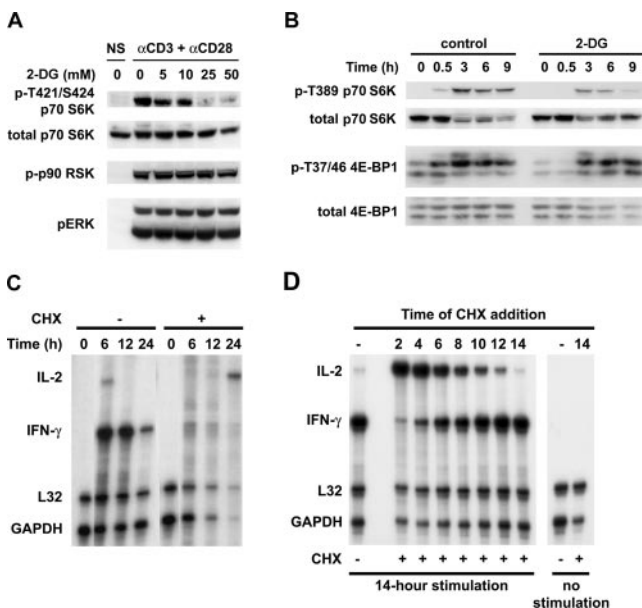


**FIGURE 5.** Protein synthesis is required for the expression of IFN- $\gamma$  mRNA. Phosphorylation of p70S6K is reduced (A) and delayed (B) in the presence of 2-DG, as determined by Western blotting. A, Effector cells were stimulated for 3 h. B, Effector cells were stimulated in 50 mM 2-DG. In some cases, the same membrane was stripped and reprobbed for the expression of other proteins. Data are representative of at least three independent experiments. C, Cycloheximide blocks IFN- $\gamma$  mRNA. Cells ( $5 \times 10^6$ ) were stimulated in the presence or the absence of cycloheximide (CHX; 10  $\mu$ g/ml) over time, as indicated. Cytokine mRNA was determined by RPA. D, To determine at what point protein synthesis was necessary for sustained IFN- $\gamma$  transcription, CHX was added at various time points during a 14-h stimulation to effector 2C CD8<sup>+</sup> T cells. Total RNA was isolated and used to measure cytokine mRNA levels by RPA. Data are representative of two independent experiments.

Together, these studies show that 2-DG can elicit either positive or negative effects on cellular immunity. Although the effect of 2-DG in those systems could be mediated through other molecules (e.g., hormones), our results suggest that 2-DG can have direct and selective effects on cytokine production by purified CD8<sup>+</sup> T cells *in vitro*.

In our current study we found no defect in DNA binding of transcription factors known to regulate IFN- $\gamma$  gene expression; however, molecular regulation of the IFN- $\gamma$  gene is incompletely understood. Recently, reporter constructs containing a -565 bp sequence upstream of the IFN- $\gamma$  gene yielded expression in Th1, but not Th2, cells (31). By contrast, transgenic T cells expressing GFP driven by a minimal 3.4-kb IFN- $\gamma$  promoter confers GFP expression in both Th1 and Th2 cells (32), arguing that this promoter does not define the factors involved in lineage-specific gene expression. A bacterial artificial chromosome transgenic mouse expressing human IFN- $\gamma$  and its upstream sequence of 191 kb was reported to be sufficient for selective expression in type 1 T cells (33), leaving open the possibility of more regulatory factors controlling IFN- $\gamma$  gene expression yet to be discovered. The T-box transcription factors, T-bet and eomesodermin, have been shown to be critical for acquisition of IFN- $\gamma$ -producing capability in CD4<sup>+</sup> and CD8<sup>+</sup> T cells (34, 35). However, recent results using dominant negative constructs have suggested that persistent function of these T-box factors is not required to retain IFN- $\gamma$  production by differentiated effector T cells (36). Whether T-bet or eomesodermin protein levels or function are dependent on glucose has not directly been determined. Our current results point toward an as yet unidentified factor that influences IFN- $\gamma$  gene expression and is dependent on glucose.

Our data showing hypophosphorylation of p70S6K and 4E-BP1 under glucose-deprived conditions along with the lack of IFN- $\gamma$  mRNA with cycloheximide treatment support the idea that *de novo* protein synthesis of at least one factor is required for IFN- $\gamma$  synthesis. However, these are correlations and do not demonstrate that p70S6K regulates IFN- $\gamma$  synthesis. In fact, rapamycin is a potent inhibitor of mammalian target of rapamycin and, therefore of p70S6K and 4E-BP1, yet does not significantly block T cell cytokine production (37, 38) (data not shown). Rather, we propose that diminished activation of p70S6K and 4E-BP1 under conditions of limiting glucose availability parallels a more complex inhibition of the process of regulated protein translation. Similar to our results, the production of the chemokine RANTES by T cells depends on the translational regulation of a transcription factor called RANTES factor of late activated T cells-1 (39). It seems likely that IFN- $\gamma$  production by CD8<sup>+</sup> T cells is regulated similarly, where an unidentified factor is required for sustained IFN- $\gamma$  transcription. Our model system should provide a means by which to identify unknown factors that regulate IFN- $\gamma$  transcription by CD8<sup>+</sup> T cells.

Our results imply that surrounding metabolic conditions may compromise CD8<sup>+</sup> effector T cell function in tissue microenvironments. T cells isolated from solid tumors often show defects in IFN- $\gamma$  production (40–42). Recently, other essential metabolites have been identified as important for T cell activation. Tryptophan appears to be essential for T cell function (43), and the enzyme IDO that degrades tryptophan is expressed in tumors (8) and can produce deleterious tryptophan metabolites that mediate T cell suppression (44, 45). T cells from tumor-bearing individuals often show deficient expression of CD3- $\zeta$  (46), which has been linked to arginase expression by cells in the tumor microenvironment (4). Because tumor cells use glucose at a higher rate than T cells (C. M. Cham and T. F. Gajewski, manuscript in press), it is conceivable that the tumor microenvironment may also be hypoglycemic. A

lack of glucose availability could contribute to the functional defects observed in tumor-isolated T cells. Although this hypothesis remains to be tested formally, preliminary results using Affymetrix gene array analysis have revealed that a subset of genes important for additional specific CD8<sup>+</sup> effector functions in addition to IFN- $\gamma$  is inhibited upon glucose deprivation (C. M. Cham and T. F. Gajewski, unpublished data). These include genes encoding granzymes, chemokines, and cell cycle molecules. It is conceivable that malignant tumor cells can adapt to these multiple metabolic derangements and that normal lymphocytes cannot, generating a major mechanism of tumor escape from T cell effector function. Thus, identifying strategies to maintain effector T cell function under conditions of limited nutrient availability could have application toward improving antitumor immunity *in vivo*.

## Acknowledgments

We thank Janel Washington for her excellent assistance with mouse breeding. We gratefully acknowledge Kenneth Frauwirth, Maria-Luisa Alegre, and Jeffrey Rathmell for stimulating discussions and experimental advice. We also thank Kenneth Frauwirth and Maria-Luisa Alegre for critically reading the manuscript.

## Disclosures

The authors have no financial conflict of interest.

## References

1. Cronin, D. C., Jr., D. W. Lancki, and F. W. Fitch. 1994. Requirements for activation of CD8<sup>+</sup> murine T cells. I. Development of cytolytic activity. *Immunol. Res.* 13:215.
2. Bird, J. J., D. R. Brown, A. C. Mullen, N. H. Moskowitz, M. A. Mahowald, J. R. Sider, T. F. Gajewski, C. R. Wang, and S. L. Reiner. 1998. Helper T cell differentiation is controlled by the cell cycle. *Immunity* 9:229.
3. Agarwal, S., and A. Rao. 1998. Modulation of chromatin structure regulates cytokine gene expression during T cell differentiation. *Immunity* 9:765.
4. Rodriguez, P. C., A. H. Zea, K. S. Culotta, J. Zabaleta, J. B. Ochoa, and A. C. Ochoa. 2002. Regulation of T cell receptor CD3 $\zeta$  chain expression by L-arginine. *J. Biol. Chem.* 277:21123.
5. Mellor, A. L., D. B. Keskin, T. Johnson, P. Chandler, and D. H. Munn. 2002. Cells expressing indoleamine 2,3-dioxygenase inhibit T cell responses. *J. Immunol.* 168:3771.
6. Rodriguez, P. C., A. H. Zea, J. DeSalvo, K. S. Culotta, J. Zabaleta, D. G. Quiceno, J. B. Ochoa, and A. C. Ochoa. 2003. L-arginine consumption by macrophages modulates the expression of CD3 $\zeta$  chain in T lymphocytes. *J. Immunol.* 171:1232.
7. Friberg, M., R. Jennings, M. Alsarraj, S. Dessureault, A. Cantor, M. Extermann, A. L. Mellor, D. H. Munn, and S. J. Antonia. 2002. Indoleamine 2,3-dioxygenase contributes to tumor cell evasion of T cell-mediated rejection. *Int. J. Cancer* 101:151.
8. Uyttenhove, C., L. Pilotte, I. Theate, V. Stroobant, D. Colau, N. Parmentier, T. Boon, and B. J. Van den Eynde. 2003. Evidence for a tumoral immune resistance mechanism based on tryptophan degradation by indoleamine 2,3-dioxygenase. *Nat. Med.* 9:1269.
9. Frauwirth, K. A., and C. B. Thompson. 2004. Regulation of T lymphocyte metabolism. *J. Immunol.* 172:4661.
10. Danial, N. N., C. F. Gramm, L. Scorrano, C. Y. Zhang, S. Krauss, A. M. Ranger, S. R. Datta, M. E. Greenberg, L. J. Licklider, B. B. Lowell, et al. 2003. BAD and glucokinase reside in a mitochondrial complex that integrates glycolysis and apoptosis. *Nature* 424:952.
11. Vander Heiden, M. G., D. R. Plas, J. C. Rathmell, C. J. Fox, M. H. Harris, and C. B. Thompson. 2001. Growth factors can influence cell growth and survival through effects on glucose metabolism. *Mol. Cell Biol.* 21:5899.
12. Rathmell, J. C., M. G. Vander Heiden, M. H. Harris, K. A. Frauwirth, and C. B. Thompson. 2000. In the absence of extrinsic signals, nutrient utilization by lymphocytes is insufficient to maintain either cell size or viability. *Mol. Cell* 6:683.
13. Ak, I., J. A. Blokland, E. K. Pauwels, and M. P. Stokkel. 2001. The clinical value of 18F-FDG detection with a dual-head coincidence camera: a review. *Eur. J. Nucl. Med.* 28:763.
14. Cham, C. M., H. Xu, J. P. O'Keefe, F. V. Rivas, P. Zagouras, and T. F. Gajewski. 2003. Gene array and protein expression profiles suggest post-transcriptional regulation during CD8<sup>+</sup> T cell differentiation. *J. Biol. Chem.* 278:17044.
15. Schreiber, E., P. Matthias, M. M. Muller, and W. Schaffner. 1989. Rapid detection of octamer binding proteins with 'mini-extracts,' prepared from a small number of cells. *Nucleic Acids Res.* 17:6419.
16. Wick, A. N., D. R. Drury, H. I. Nakada, and J. B. Wolfe. 1957. Localization of the primary metabolic block produced by 2-deoxyglucose. *J. Biol. Chem.* 224:963.



17. Lancki, D. W., C. S. Hsieh, and F. W. Fitch. 1991. Mechanisms of lysis by cytotoxic T lymphocyte clones: lytic activity and gene expression in cloned antigen-specific CD4<sup>+</sup> and CD8<sup>+</sup> T lymphocytes. *J. Immunol.* 146:3242.
18. Yoshimoto, T., H. Okamura, Y. I. Tagawa, Y. Iwakura, and K. Nakanishi. 1997. Interleukin 18 together with interleukin 12 inhibits IgE production by induction of interferon- $\gamma$  production from activated B cells. *Proc. Natl. Acad. Sci. USA* 94:3948.
19. Yang, J., H. Zhu, T. L. Murphy, W. Ouyang, and K. M. Murphy. 2001. IL-18-stimulated GADD45 $\beta$  required in cytokine-induced, but not TCR-induced, IFN- $\gamma$  production. *Nat. Immunol.* 2:157.
20. Rincon, M., H. Enslen, J. Raingeaud, M. Recht, T. Zapton, M. S. Su, L. A. Penix, R. J. Davis, and R. A. Flavell. 1998. Interferon- $\gamma$  expression by Th1 effector T cells mediated by the p38 MAP kinase signaling pathway. *EMBO J.* 17:2817.
21. Penix, L. A., M. T. Sweetser, W. M. Weaver, J. P. Hoefler, T. K. Kerppola, and C. B. Wilson. 1996. The proximal regulatory element of the interferon- $\gamma$  promoter mediates selective expression in T cells. *J. Biol. Chem.* 271:31964.
22. Dennis, P. B., A. Jaeschke, M. Saitoh, B. Fowler, S. C. Kozma, and G. Thomas. 2001. Mammalian TOR: a homeostatic ATP sensor. *Science* 294:1102.
23. Frauwirth, K. A., J. L. Riley, M. H. Harris, R. V. Parry, J. C. Rathmell, D. R. Plas, R. L. Elstrom, C. H. June, and C. B. Thompson. 2002. The CD28 signaling pathway regulates glucose metabolism. *Immunity* 16:769.
24. Boise, L. H., A. J. Minn, P. J. Noel, C. H. June, M. A. Accavitti, T. Lindsten, and C. B. Thompson. 1995. CD28 costimulation can promote T cell survival by enhancing the expression of Bcl-x<sub>L</sub>. *Immunity* 3:87.
25. Chakrabarti, R., C. Y. Jung, T. P. Lee, H. Liu, and B. K. Mookerjee. 1994. Changes in glucose transport and transporter isoforms during the activation of human peripheral blood lymphocytes by phytohemagglutinin. *J. Immunol.* 152:2660.
26. Pascoe, W. S., G. A. Smythe, and L. H. Storlien. 1989. 2-Deoxy-D-glucose-induced hyperglycemia: role for direct sympathetic nervous system activation of liver glucose output. *Brain Res.* 505:23.
27. Cato, R. K., L. M. Flanagan, J. G. Verbalis, and E. M. Stricker. 1990. Effects of glucoprivation on gastric motility and pituitary oxytocin secretion in rats. *Am. J. Physiol.* 259:R447.
28. McCaleb, M. L., and R. D. Myers. 1982. 2-Deoxy-D-glucose and insulin modify release of norepinephrine from rat hypothalamus. *Am. J. Physiol.* 242:R596.
29. Dreau, D., D. S. Morton, M. Foster, N. Fowler, and G. Sonnenfeld. 2000. Effects of 2-deoxy-D-glucose administration on cytokine production in BDF1 mice. *J. Interferon Cytokine Res.* 20:247.
30. Miller, E. S., R. A. Bates, D. A. Koebel, B. B. Fuchs, and G. Sonnenfeld. 1998. 2-Deoxy-D-glucose-induced metabolic stress enhances resistance to *Listeria monocytogenes* infection in mice. *Physiol. Behav.* 65:535.
31. Soutto, M., F. Zhang, B. Enerson, Y. Tong, M. Boothby, and T. M. Aune. 2002. A minimal IFN- $\gamma$  promoter confers Th1 selective expression. *J. Immunol.* 169:4205.
32. Zhu, H., J. Yang, T. L. Murphy, W. Ouyang, F. Wagner, A. Saparov, C. T. Weaver, and K. M. Murphy. 2001. Unexpected characteristics of the IFN- $\gamma$  reporters in nontransformed T cells. *J. Immunol.* 167:855.
33. Soutto, M., W. Zhou, and T. M. Aune. 2002. Cutting edge: distal regulatory elements are required to achieve selective expression of IFN- $\gamma$  in Th1/Tc1 effector cells. *J. Immunol.* 169:6664.
34. Szabo, S. J., S. T. Kim, G. L. Costa, X. Zhang, C. G. Fathman, and L. H. Glimcher. 2000. A novel transcription factor, T-bet, directs Th1 lineage commitment. *Cell* 100:655.
35. Pearce, E. L., A. C. Mullen, G. A. Martins, C. M. Krawczyk, A. S. Hutchins, V. P. Zediak, M. Banica, C. B. DiCioccio, D. A. Gross, C. A. Mao, et al. 2003. Control of effector CD8<sup>+</sup> T cell function by the transcription factor Eomesodermin. *Science* 302:1041.
36. Mullen, A. C., A. S. Hutchins, F. A. High, H. W. Lee, K. J. Sykes, L. A. Chodosh, and S. L. Reiner. 2002. Hlx is induced by and genetically interacts with T-bet to promote heritable T<sub>H</sub>1 gene induction. *Nat. Immunol.* 3:652.
37. Bierer, B. E., P. S. Mattila, R. F. Standaert, L. A. Herzenberg, S. J. Burakoff, G. Crabtree, and S. L. Schreiber. 1990. Two distinct signal transmission pathways in T lymphocytes are inhibited by complexes formed between an immunophilin and either FK506 or rapamycin. *Proc. Natl. Acad. Sci. USA* 87:9231.
38. Dumont, F. J., M. J. Staruch, S. L. Koprak, M. R. Melino, and N. H. Sigal. 1990. Distinct mechanisms of suppression of murine T cell activation by the related macrolides FK-506 and rapamycin. *J. Immunol.* 144:251.
39. Nikolcheva, T., S. Pyronnet, S. Y. Chou, N. Sonenberg, A. Song, C. Clayberger, and A. M. Krensky. 2002. A translational rheostat for RFLAT-1 regulates RANTES expression in T lymphocytes. *J. Clin. Invest.* 110:119.
40. Roussel, E., M. C. Gingras, E. A. Grimm, and J. A. Roth. 1995. High expression of adhesion molecules/activation markers with little interleukin-2, interferon  $\gamma$ , and tumor necrosis factor  $\beta$  gene activation in fresh tumor-infiltrating lymphocytes from lung adenocarcinoma. *Cancer Immunol. Immunother.* 41:1.
41. Guilloux, Y., C. Viret, N. Gervois, E. Le Drean, M. C. Pandolfino, E. Diez, and F. Jotereau. 1994. Defective lymphokine production by most CD8<sup>+</sup> and CD4<sup>+</sup> tumor-specific T cell clones derived from human melanoma-infiltrating lymphocytes in response to autologous tumor cells in vitro. *Eur. J. Immunol.* 24:1966.
42. Blohm, U., E. Roth, K. Brommer, T. Dumrese, F. M. Rosenthal, and H. Pircher. 2002. Lack of effector cell function and altered tetramer binding of tumor-infiltrating lymphocytes. *J. Immunol.* 169:5522.
43. Mellor, A. L., P. Chandler, G. K. Lee, T. Johnson, D. B. Keskin, J. Lee, and D. H. Munn. 2002. Indoleamine 2,3-dioxygenase, immunosuppression and pregnancy. *J. Reprod. Immunol.* 57:143.
44. Terness, P., T. M. Bauer, L. Rose, C. Dufter, A. Watzlik, H. Simon, and G. Opelz. 2002. Inhibition of allogeneic T cell proliferation by indoleamine 2,3-dioxygenase-expressing dendritic cells: mediation of suppression by tryptophan metabolites. *J. Exp. Med.* 196:447.
45. Frumento, G., R. Rotondo, M. Tonetti, G. Damonte, U. Benatti, and G. B. Ferrara. 2002. Tryptophan-derived catabolites are responsible for inhibition of T and natural killer cell proliferation induced by indoleamine 2,3-dioxygenase. *J. Exp. Med.* 196:459.
46. Mizoguchi, H., J. J. O'Shea, D. L. Longo, C. M. Loeffler, D. W. McVicar, and A. C. Ochoa. 1992. Alterations in signal transduction molecules in T lymphocytes from tumor-bearing mice. *Science* 258:1795.